





Received December 9, 2021, accepted December 23, 2021, date of publication December 28, 2021, date of current version January 4, 2022.

Digital Object Identifier 10.1109/ACCESS.2021.3139075

Improved Cycle Aging Cost Model for Battery Energy Storage Systems Considering More Accurate Battery Life Degradation

LEIQI ZHANG¹, YANJIE YU¹, BO LI², (Student Member, IEEE), XIAO QIAN³, SHUJUN ZHANG³, XIANGJIN WANG¹, XUESONG ZHANG¹, AND MINYOU CHEN², (Senior Member, IEEE)

¹State Grid Zhejiang Electric Power Research Institute, Hangzhou, Zhejiang 310000, China

²School of Electric Engineering, Chongqing University, Chongqing 400030, China

³State Grid Zhejiang Electric Power Company, Hangzhou, Zhejiang 310000, China

Corresponding author: Bo Li (boli9301@163.com)

This work was supported by the Science and Technology Project of State Grid Zhejiang Electric Power Company of China under Grant 5211DS19002F.

ABSTRACT Battery energy storage systems (BESSs) have been widely used in power grids to improve their flexibility and reliability. However, the inevitable battery life degradation is the main cost in BESS operations. Thus, an accurate estimation of battery aging cost is strongly needed to cover the actual cost of BESSs. The existing models of battery life degradation either are not fully accurate to estimate the actual cost or are not solved easily because of their computation nonlinearity. In this paper, a piece-wise linear battery aging cost model with an accurate estimate of battery life degradation for BESSs is proposed to extend battery life and improve battery profits. In our method, the widely-used Arrhenius law is modified to quantify the battery life degradation affected by the depth of cycle. Further, a nonlinear battery cycle aging cost model is developed by finding the derivative of battery life degradation with respect to discharging power, which indicates the battery life degradation rate due to depth of cycle. To reduce the complexity of computation, a piece-wise linearization method is proposed to simplify the battery cycle aging cost model. Finally, the cycle aging cost model with an accurate estimation of battery life degradation is applied to the optimization dispatch in the day-ahead energy and auxiliary service market. The results show that the error of estimating the battery cycle aging cost of BESSs is less than 5% under proper piece-wise segment numbers. The profits are increased by 27% and the battery life is extended by 11% than the fixed cost method.


INDEX TERMS Battery energy storage system, piece-wise linear model, cycle aging cost, state of health, optimization dispatch.

I. INTRODUCTION

Due to dramatic cost reduction in wind and solar photovoltaic (PV), renewable energy is being increasingly incorporated into power grids [1], [2]. The uncertainty and intermittent of renewable energy generation considerably affect the security operation of power grids [3]. Energy storage technologies are promising options to address these intermittency and uncertainty problems of renewable energy generation through daily and multi-day energy shifting under high penetration of renewable energy [4]. BESSs are experiencing increasingly

being used in various grid-scale applications due to technology development and incentive policies [5]–[8]. BESS could furnish the deficit power in renewable energy power forecasting because of the prediction error [9] and could be applied to determine the best operating strategy of the cluster of multi-hybrid wind farms [10]. Unlike traditional power generation plants, the lifetime of BESSs resulting from aging degradation is highly sensitive to BESS types and dispatch strategies [11].

The aging of BESS mainly results from the formation of the solid electrolyte interface (SEI), leading to an increase in the internal resistance and battery life degradation of BESSs [12], [13]. Two common BESSs aging methods

The associate editor coordinating the review of this manuscript and approving it for publication was Dipankar Deb .

quantify the BESS degradation process: calendar aging and cycle aging [14]. Calendar aging of batteries primarily occurs during the energy storage phase of the battery, mainly resulting from the state of charge (SOC) and the temperature of the battery [15]–[18]. When the energy is stored in a battery, the formation of SEI will generate due to the reduction of electrolyte solvents such as ethylene carbonate [19], [20]. Cycle aging of BESS is affected by kinetic factors related to charging and discharging cycle operating parameters including charging/discharging rate, depth of cycle, cycle number, and operating temperature [21]–[24]. Further, cycle aging is primarily affected by the cycle number and the depth of cycle [25], [26]. Incorporating an accurate battery cycle aging estimation method into BESSs short-term operational decisions is important to improve the longevity and profitability of the battery.

There are two main semi-empirical aging models to estimate the cycle aging of BESS. 1) Based on the semi-empirical model of Arrhenius law, the relationship between battery cycle aging and time is established by involving diffusion and parasitic reactions leading to loss of active lithium [27]. It clearly indicates the correlation parameters in battery operations and is applied to calculate the cost of BESSs [28]. Fitting parameters are directly from the battery mechanism data under given conditions. Additionally, this model could apply to most kinds of BESSs through cell life experiments. Hence, this model is used widely in battery mechanism research. While the main weakness of the model based on the Arrhenius law is that cycle aging is affected by two interactive variables, which indicates that it could be not easily implemented in the optimization dispatch. 2) Based on quadratic cycle depth stress function, the relationship between the depth of cycle and the degree of cycle aging is established through the radius of active material degradation in the battery profile [29]. In this case, the depth of cycle directly affects the battery cycle aging. This model can be easily incorporated in optimization dispatch. However, this method usually needs numerous mechanism experiments to obtain fitting parameters. The radius of active material is also difficult to measure during the experiment [30]. Consequently, the models mentioned above either are not fully accurate to reflect the actual cost of BESS or are not implemented in optimization dispatch easily.

Despite the above documented two main semi-empirical aging models, there exists no explicit or rigorous way to incorporate the aging model into optimization dispatch. BESS have different performance characteristics and grid-scale applications, such as arbitrage and regulation service. When participating in grid-scale applications, BESS operators need to optimize the daily charging/discharging power dispatch to maximize profits. Besides, they need to account for the cycle aging of BESSs to extend service life. For instance, the threshold battery power level is set to avoid a large number of charging and discharging cycles [31]. Based on the fuzzy multi-criteria decision-making techniques, this operating strategy could avoid excessive battery

degradation significantly. Unlike traditional thermal generators that have variables to estimate the operating cost, the aging cost of a battery is difficult to predict as it consumes no fuel. An adaptive control law is developed to compensate for the uncertain parameter related to the SOC and open-circuit voltage [32]. The damage equivalent quantity (DEQ), which indicates a depth of discharge value for the predefined number of battery cycles, could be applied to the suitable dispatch regulator and forecasting scheme to minimize the operating cost of hybrid wind energy systems [33]. The battery aging cost of BESS is ignored in dispatch objective function in many studies [34], [35], or is not explained or justified why the cost function is implemented [36], [37]. Most researchers have applied fixed cost in battery cost calculation [38], [39]. In those optimization dispatches implemented BESSs in power systems, they assume that the battery degradation is proportional to the cycle numbers roughly while considering the degradation cost of BESS [40]–[42]. The main weakness of this method is that it would underestimate the actual aging cost of the battery, due to ignoring the fact that deep depth of cycle would accelerate the cycle aging of the battery, and resulting that battery reaches the end of life (EOL) too early. Furthermore, researchers regard maximum battery life as the optimization goal [43]. In this model, the profits could not be maximized and the efficiency of BESSs would be reduced by low depth of cycle.

This study proposed an improved cycle aging cost model of BESS considering battery aging based on the Arrhenius law to accurately estimate the BESS cycle aging cost. Additionally, a piece-wise linear model is implemented to approximate the actual battery aging model in order to optimization dispatch. The proposed model was used in a BESS dispatch problem to optimize battery longevity and profitability. The main contributions of this paper are as follows:

- 1) It proposes a single-variable battery cycle aging model based on Arrhenius law to quantify the relationship between the depth of cycle and battery capacity degradation. The proposed method allows the cycle aging model could be incorporated in optimization dispatch.

- 2) The battery capacity degradation is associated with the discharging power, which is derived from the single-variable model.

- 3) Since the nonlinear function above could not be simply incorporated in optimization dispatch, the piece-wise linear method is implemented into the battery cycle aging model to approximate the actual battery cycle aging function.

- 4) The accuracy of the proposed model increases with the increasing linearization segments. The results of BESS optimization dispatch in energy and auxiliary service markets demonstrated the improvements in profitability and longevity of the battery.

The paper is organized as follows. Section II describes the formulation of the cycle aging cost model of the BESS based on the Arrhenius law. Section III details how this model is incorporated in the economic optimization dispatch and

the dispatch objective function and constraints. Section IV discusses the accuracy and the improvement of the proposed model. Section V draws the conclusion.

II. AGING COST MODEL OF BESS CONSIDERING BATTERY LIFE DEGRADATION

A. BATTERY CYCLE AGING MODEL BASED ON ARRHENIUS LAW

Arrhenius law could effectively reflect the chemical reaction rate by factors in conditions of a small range of temperature [44]. The charging/discharging process of BESS is a chemical reaction process, which can be solved by using the Arrhenius law as follows [27]:

$$Q_{loss} = A \exp\left(\frac{-E_a}{RT}\right) \mu^z \quad (1)$$

where Q_{loss} is the capacity fade of battery (%); A is the Arrhenius constant; z is the reaction rate constant; R is the molar gas constant (J/(mol·K)); E_a is the activation energy (J/mol); T is the absolute temperature (K), and μ is chemical time (hr). The variable A_h could be introduced instead of μ [19]. A_h is the Ah-throughput which allows us to correlate the battery degradation with cycle numbers and depth of cycle:

$$A_h = E_{rate} \times n \times h \quad (2)$$

where E_{rate} is the capacity of the battery (MWh); n is the cycle number; h is the depth of the cycle. When the battery capacity is fixed, A_h is affected by the two factors at the same time; μ can be substituted from (2). Thus, the following cycle aging model of the BESS is proposed:

$$\begin{aligned} Q_{loss}(n, h) &= A \exp\left(\frac{-E_a}{RT}\right) A_h^z \\ &= A \exp\left(\frac{-E_a}{RT}\right) (E_{rate} \times n \times h)^z \end{aligned} \quad (3)$$

After battery material and operating environment are determined, two unknown coefficients A and z could be obtained. To determine the fitting parameters A and z , (3) is transformed as follows:

$$\begin{aligned} \ln(Q_{loss}) &= \ln(A) - \left(\frac{E_a}{RT}\right) + z \ln(A_h) \\ \ln(Q_{loss}) + \left(\frac{E_a}{RT}\right) &= z \ln(A_h) + \ln(A) \end{aligned} \quad (4)$$

where A and z could be obtained by linear programming. The cycle number n and depth of the cycle h under different operating temperatures could be obtained by materials stress experiments. Then the regression function could be plotted between $\ln(A_h)$ and $\ln(Q_{loss}) + E_a/RT$. The value of A was obtained from the intercept values of the best-fit nonlinear regression function; z was obtained from the slope of the curves [19]. Here, linear programming could be incorporated to fix the model. Furthermore, A_h follows the Arrhenius law because the generation of the aging layer is a chemical reaction of the battery during thermal activation [45].

The degree of cycle aging of the battery in a period can be estimated by using the state of life (SoH) [12], [46] formulated as follow:

$$\text{SoH} = 1 - \frac{Q_{loss,t}}{Q_{rated}} \quad (5)$$

where SoH represents the life degradation of the battery at various moments; $Q_{loss,t}$ is the capacity degradation of the battery at t (MWh); Q_{rated} is the initial capacity of the battery (MWh).

B. CYCLE AGING COST MODEL CONSIDERING THE BATTERY LIFE DEGRADATION

According to the BESS battery degradation in Section A, the cycle aging of the battery is affected by both the depth of cycle h and the cycle number n when the battery material and operating environment are determined. Equation (3) could not be implemented into optimization dispatch of BESSs, because it cannot intuitively reflect the relationship between cycle aging and the depth of cycle. To quantify the battery cycle aging in one cycle, (3) could be transformed into a single-variable formulation:

$$Q_{cycle}(h) = A \exp\left(\frac{-E_a}{RT}\right) (hE_{rate})^z \quad (6)$$

where $Q_{cycle}(h)$ is capacity degradation for one cycle.

This study did not consider the battery capacity degradation caused by the battery during the discharging state of a cycle, this assumption is reasonable because the amounts of energy are almost identical due to the same initial and ending SOC. Therefore, the cycle aging of the battery was assumed to only occur during the battery discharging stage of a cycle.

The cycle depth is the amount of change in the SOC of the battery during discharging [41]. During the battery cycle, the stored energy is discharged from the start energy e^{up} to the end energy e^{dn} , then h is $(e^{up} - e^{dn})/E^{rate}$. If the battery is discharged at intervals t , then the relationship between h_t and P_t^{dis} at t can be expressed as follows:

$$h_t = \frac{1}{\eta^{dis} E_{rate}} P_t^{dis} \Delta t \quad (7)$$

where η^{dis} is the battery discharge efficiency (%); P_t^{dis} is the discharging power of battery at t (MW), and h_t is the depth of cycle at t (%). To determine the relationship between discharging power P_t^{dis} and battery capacity degradation Q_{loss} , the partial derivative can be calculated by (6) [26], and the process can be expressed as follows:

$$\begin{aligned} \frac{\partial Q_{loss}(n_t, h_t)}{\partial P_t^{dis}} &= \frac{\partial Q_{loss}(n_t, h_t)}{\partial h_t} \frac{dh_t}{dP_t^{dis}} \\ &= \frac{1}{\eta^{dis} E_{rate}} \frac{\partial Q_{loss}(n_t, h_t)}{\partial h_t} \end{aligned} \quad (8)$$

where n_t is the cycle number of the battery at time t ; $dQ_{loss}(n_t, h_t)/dh_t$ is the derivative of battery capacity degradation to the depth of cycle, that is, the rate of change of cycle depth to battery life degradation, which can be considered

as the effect of each unit depth of cycle on battery life under a single cycle. Therefore, (6) can be used instead of $dQ_{loss}(n_t, h_t)/dh_t$ as follows:

$$\frac{\partial Q_{loss}(n_t, h_t)}{\partial h_t} = Q_{cycle}(h_t) = A \exp\left(\frac{-E_a}{RT}\right) (h_t E_{rate})^z \quad (9)$$

where the right side of (9) is the cycle aging caused by the depth of the cycle under a single cycle, Table 1 shows the fitting parameters of the LiFePO4 battery[19]. Thus, the relationship between the cycle life of the battery and the output power can be obtained. The cost of a certain discharging degradation of the battery can be expressed as follows:

$$\omega = \frac{C}{\eta^{dis} E_{rate}} Q_{cycle}(h_t) \quad (10)$$

where ω is the cost for battery cycle aging, P_t^{dis} is the discharging power at time t (MW), and C is the replacement cost (\$). The cycle aging cost of the battery under various cycle depths in a single cycle can be calculated according to (10).

TABLE 1. Battery fitting parameters.

Type	A	$E_a(J/mol)$	$R(J/(mol \cdot K))$	z
LiFePO ₄	330,330	-31,500	8.314	0.552

C. BATTERY PIECE-WISE LINEARIZATION MODEL

Equation (6) represents the calculation formulation of battery aging cost. However, solving the nonlinear function $Q_{cycle}(h_t)$ is difficult. Conventional linearization methods tend to exhibit large deviations. Therefore, this study proposed a piecewise linearization model that enables the energy storage degradation cost model to be embedded in the conventional unit commitment or economic dispatch model to improve the efficiency of the solution.

The independent variable is h_t in nonlinear $Q_{cycle}(h_t)$. Therefore, the depth of cycle is divided into segments, as displayed in Fig. 1.

In Fig. 1, the capacity degradation is plotted as a function of the depth of cycle. The mid-value of each segment represents the whole segment value. More segments make the approximate function closer to the original function (e.g., between S2 and S3). Thus, the piece-wise linear model can be expressed as follows:

$$\omega(h_t) = \omega_i \text{ if } h_t \in \left[\frac{i-1}{N}, \frac{i}{N}\right), \quad i = 1, 2, \dots, N \quad (11)$$

$$\omega_i = \frac{R}{\eta^{dis} E_{rate}} k_i \quad (12)$$

$$k_i = \frac{1}{2} \left[Q_{cycle}\left(\frac{i}{N}\right) - Q_{cycle}\left(\frac{i-1}{N}\right) \right] \quad (13)$$

where N is the total number of segments; i is the number of segments where the current depth of cycle is located;

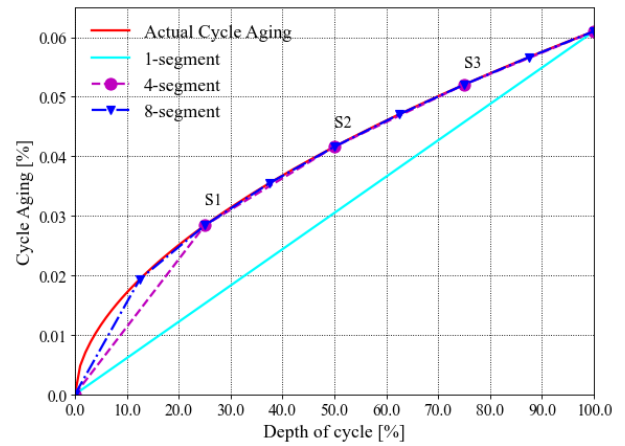


FIGURE 1. Piece-wise linear model for cycle life degradation of energy storage batteries.

ω is a piece-wise linear approximation function; k is the mid-value in the current segment. In this paper, the depth of cycle is calculated by segments in the optimization process to reduce the deviation. Therefore, the output power corresponding to the depth of cycle should be calculated by segments.

III. BESS DISPATCH MODEL

This study implemented the established linear aging cost model of the battery into the day-ahead energy and auxiliary service market, which can be expressed as follows:

$$\max_{P,R} \Phi = \sum_{t=1}^T \Delta t \left[\sigma_t^P (P_t^{dis} - P_t^{ch}) + \sigma_t^Q R_t \right] - W \quad (14)$$

$$W = \sum_{t=1}^T \sum_{i=1}^N \Delta t \omega_i P_{t,i}^{dis} \quad (15)$$

where Δt is the time interval, T is the number of time intervals in optimization index by t ; Φ is the revenue of the battery in optimization dispatch (\$); σ_t^P and σ_t^Q are the energy and reserve price at t (\$/MW), respectively; W is the cycle aging cost in a single optimization dispatch cycle, N is the segments of piece-wise linear aging cost model of battery index by i ; ω_i is the mid-value in the segment i ; P_t^{dis} and P_t^{ch} are the discharging and charging power of battery at t (MW), respectively; R_t is the reserve power of battery at t (MW); $P_{t,i}^{dis}$ and $P_{t,i}^{ch}$ are the discharging and charge power of the battery in segment i at t (MW), respectively.

Constraints can be expressed as follows:

(1) Battery power constraints are as follows:

$$P_t^{dis} = \sum_{i=1}^N P_{t,i}^{dis} \quad (16)$$

$$P_t^{ch} = \sum_{i=1}^N P_{t,i}^{ch} \quad (17)$$

$$0 \leq P_t^{dis} \leq x_{t,1} P_{\max}^{dis} \quad (18)$$

$$0 \leq P_t^{ch} \leq x_{t,2} P_{\max}^{ch} \quad (19)$$

$$x_{t,k} \in \{0, 1\} \quad (20)$$

$$\sum_{k=1}^3 x_{t,k} = 1, \quad \forall t \quad (21)$$

where P_{\max}^{dis} and P_{\max}^{ch} are the maximum discharging and charging power of the battery (MW), respectively; $x_{t,k}$ is the logical variable; k represents discharging, charging, and reserve when it is 1, 2, and 3 respectively. Constraints (16) and (17) state that BESS power is the summation of the discharging/charging power associated with each cycle depth segment, respectively; Constraints (18) and (19) are for battery discharging and charging power, respectively. Constraints (20) and (21) indicate that energy storage can only be charged, discharged, and reserved at a certain time.

(2) Battery energy storage constraint

$$E_{t,i} = E_{t-1,i} + p_{t,i}^{ch} \eta^{ch} \Delta t - \frac{p_{t,i}^{dis} \Delta t}{\eta^{dis}} \quad (22)$$

$$E_{\min} \leq \sum_{i=1}^N E_{t,i} \leq E_{\max} \quad (23)$$

$$E_t = \sum_{i=1}^N E_{t,i} \quad (24)$$

$$E_1 = E_N \quad (25)$$

$$E_{t,i} \geq 0 \quad (26)$$

$$E_t^R \leq \beta E_t \quad (27)$$

$$0 \leq R_t \Delta t \leq E_t^R \quad (28)$$

$$0 \leq \beta < 1 \quad (29)$$

where $E_{t,i}$ is the energy storage in segment i at t (MWh); E_{\min} and E_{\max} are the maximum and minimum energy storage of battery (MWh); E_t is the energy storage at t (MWh); η^{dis} and η^{ch} is the efficiency of battery discharging and charging (%), respectively; E_t^R is reserve energy at t (MWh); β is the ratio of energy for reserve at t . Equation (22) is the constraints on the evolution of the energy stored in each cycle depth segment between t and $t-1$; Equation (23) is energy storage constraint; Equation (24) is sum constraint for energy, the sum of the energy of the battery under each cycle depth i at t is equal to the total energy at t ; Equation (25) is the initial and final capacity constraints of the battery. In this study, the initial power of the battery in a period is set to be the same as the final power at the end of optimization dispatch. Equation (27) indicates the reserve energy constraints. Equation (28) indicates the reserve energy constraint of the battery at t .

Fig. 2 is the illustration of BESS incorporated in optimization dispatch. For BESS optimization dispatch, first, an improved single-variable cycle aging function of the battery should be established based on the fitting parameters provided by the battery manufacturer or the battery parameters. Second, the battery model is improved according to the piece-wise linear method proposed in this paper. Third, the dispatch is optimized based on day-ahead energy and auxiliary service market. Finally, dispatch profile and profit analysis are conducted.

IV. CASE STUDY

The proposed cycle aging cost model of the battery was incorporated in the day-ahead energy and auxiliary services market to prove the effectiveness of the model. In this case, BESS will charge/discharge frequently to energy arbitrage or

reserve, so different segments of the piece-wise linear aging cost model were implemented to verify the accuracy of the proposed model. The results also indicate the model proposed improves the profitability and longevity of BESS.

A. DATA DESCRIPTION

In this case study, the day-ahead locational marginal price (LMP) and auxiliary services price was derived from the Pennsylvania—New Jersey—Maryland (PJM) day-ahead market. All simulations were modeled and solved in the MATLAB platform using YALMIP and CPLEX in one year. BESS operating parameters are displayed in Table 2 [26].

TABLE 2. The battery operating parameters.

Type	LiFePO ₄ Battery
Charge and discharge rated power	10 MW
Capacity	20 MWh
Charge and discharge efficiency	95%
Maximum SOC	95%
Minimum SOC	15%
Battery replacement cost	300,000\$/MWh
Operating temperature	25°C
Battery shelf life	10 years

B. RESULTS OF CYCLE AGING COST MODEL UNDER DIFFERENT SEGMENTS

To demonstrate the profitability and longevity of the cycle aging cost model under piece-wise linear aging cost models with various segments, this study implemented 1-segment, 8-segment, 64-segment, and models with zero operating cost of BESS into the optimization. Assumption of the model with zero operating cost indicates BESSs have no cost due to discharging/charging phase. The 1-segment model is the widely used fixed cost model of battery. Fig. 3 (a) shows the optimization dispatch curve of the piece-wise linear cycle aging cost model under different segments in a certain day. Fig. 3 (b) shows the LMP and reserve price in a certain day. It illustrates that various segments model of BESSs both tend to charge at low LMP in a period of 6:00-10:00 to increase the SOC of battery, then reserve the energy to provide the auxiliary services with stable SOC. Whole numbers of segments model of BESSs both tend to discharge at high LMP in period 20:00-22:00 to arbitrage. The SOC of BESS ramps most aggressively under the model with zero operating cost. The maximum SOC of BESS under the 1-segment model is less than those of the zero operating cost model because arbitrage will be limited by cycle aging cost. In addition, the maximum SOC of BESS decreases as the increasing numbers of segments due to a more accurate estimation of cycle aging cost, which results in more cycle aging costs at the same discharging/charging power. Consequently, as the numbers of segments increase, BESS will arbitrage conservatively, the maximum SOC of BESS will decrease at the same time.

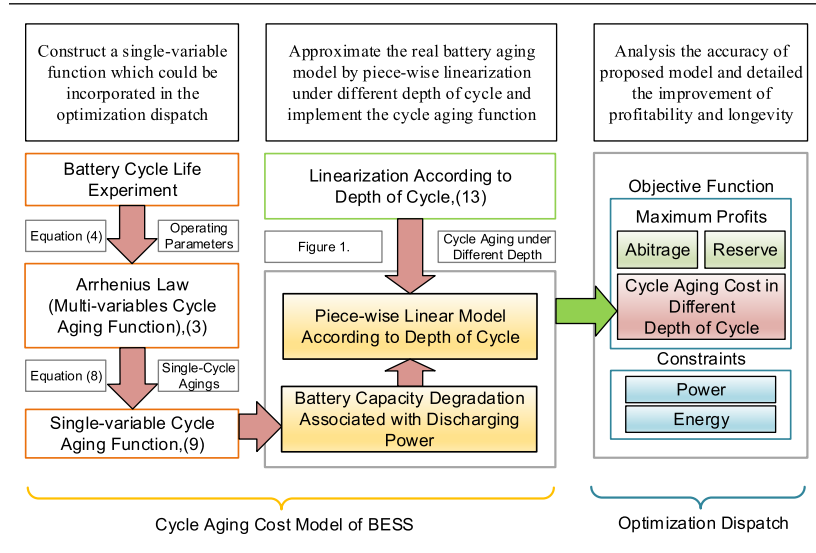


FIGURE 2. The illustration of BESS incorporated in optimization dispatch.

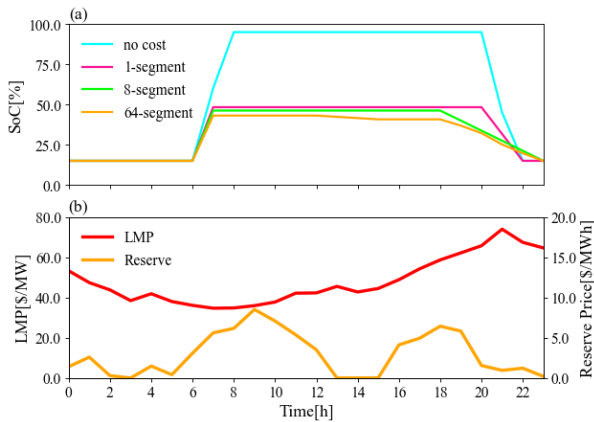


FIGURE 3. (a) The optimization dispatch curve of piece-wise cycle linear aging cost model. (b) LMP and reserve price in a certain day.

C. ANALYSIS OF RESULTS

1) METRICS OF COMPARISON

In order to quantify the approximation to the accurate cycle aging cost of BESSs, we compute the relative error as follows

$$\varepsilon = \frac{|\tilde{Q}_{loss} - Q_{loss}|}{Q_{loss}} \quad (30)$$

where ε is the relative error, Q_{loss} is the accurate cycle aging cost of BESS by (3), \tilde{Q}_{loss} is the actual cycle aging cost estimated by the proposed model in this paper.

The piece-wise linear cycle aging cost model can estimate the cycle aging cost of BESS accurately with enough numbers of segments because more numbers of segments make the approximate function closer to the original function (e.g., between S2 and S3) in Fig. 1. Fig. 4 shows the errors of the piece-wise linear model versus the accurate estimation, regarding the accurate cycle aging cost as the benchmark.

The error decreases from 77.8% under 1-segment model to 0.02% under 288-segment model. The results indicate that the proposed model achieved the best cost approximation. Notably, more segments may reduce the efficiency of solving. The BESS operator should minimize the number of segments under the premise of meeting the relative error requirement in practice because the relative error is only 2% under the 64-segment model.

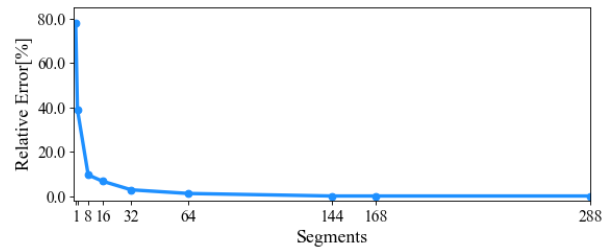


FIGURE 4. Error comparisons of simplified BESS cycle aging cost model under different numbers of segments.

2) BESS PROFITABILITY ANALYSIS

The cycle aging cost of the battery has an impact on the profits of BESS. Table 3 shows the profits and costs of BESS under different numbers of segments in the day-ahead energy and auxiliary services market. The annual arbitrage profit of the model with zero operating cost is \$368.1 thousand which is far beyond other situations considering the cycle aging cost. The actual annual cycle aging cost of this model reaches \$2320.0 thousand, which is 20~40 times than situations considering the cycle aging cost. Although the arbitrage profits of this model are maximum, the total profits of that are the minimum. The annual total profit is \$-1929.6 thousand. The BESS with zero operating cost is the most aggressive dispatch and the BESS tends to arbitrage as much possible

as the fluctuation of LMP with the rated power. This leads to the largest cycle aging cost of BESS. With the number of segments increasing, the cycle aging cost model proposed of BESS can effectively improve the profits in optimization dispatch. The annual total profits increased from \$42.4 thousand under the 1-segment cycle aging cost model of BESS to \$53.9 thousand under the 64-segment model. Specifically, the annual arbitrage profits decreased from \$136.1 thousand under the 1-segment model to \$93.4 thousand under the 64-segment model due to the more conservative arbitrage choices with the increasing numbers of segments. The annual auxiliary services profits decreased from \$24.7 thousand under the 1-segment model to \$18.6 thousand under the 64-segment model due to the smaller discharging/charging power. The smaller power reduces the energy storage of BESS. The actual annual cycle aging costs can be estimated by (15) decreasing from \$118.4 thousand under the 1-segment model to \$58.1 thousand under the 64-segment model. Thus, the proposed model can effectively reduce the cycle aging costs of BESSs by 50% and improve the total profits by 27% than the 1-segment model.

TABLE 3. The annual profits and costs of BESS under different numbers of segments in the day-ahead energy and auxiliary services market.

Number of Segments	No Cost	1-segment	8-segment	64-segment
Annual Total Profit/k\$	-1929.6	42.4	49.3	53.9
Annual Arbitrage Profit/k\$	368.1	136.1	107.1	93.4
Annual Auxiliary Service Profit/k\$	22.3	24.7	20.6	18.6
Actual Annual Cycle Aging Cost/k\$	2320.0	118.4	78.4	59.1

3) BESS LONGEVITY ANALYSIS

Fig. 5 shows the SoH of BESS under different numbers of segments in the energy and auxiliary service market over one year. It is noted that a one-year simulation is divided into 12-month simulations due to computation complexity. After one year of operation, the SoH of BESS decreased from 100% to approximately 99.0% under the 64-segment model, compared with the value of 97.8% under the 1-segment model. Thus, the increasing number of segments can reduce the battery life degradation and improve the longevity of BESS. Additionally, the SoH of the model with zero operating cost decreases fastest in the simulation. Consequently, the proposed model can extend the battery life to reduce the replacement cost and prevent BESS from reaching the EOL.

It is worth emphasizing that the high segments lead to a conservative arbitrage choice of BESS. Fig. 6 illustrates the discharging/charging power profiles of BESS in the energy and auxiliary service market. The maximum charging/discharging power under the model with zero operating cost

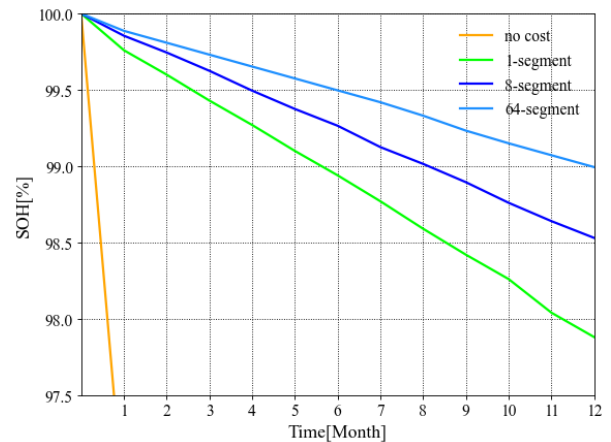


FIGURE 5. The SoH of BESS under different numbers of segments in the energy and auxiliary service market over one year.

is the largest. The BESS would arbitrage more aggressively with full power at zero cost, but it would lead to a higher cycle aging cost in actuality. After integrating the proposed model, BESS would not tend to arbitrage at full power to reduce the battery life degradation. Further, the maximum discharging/charging power of the 1-segment model is higher than the 8-segment and 64-segment model, which is bound to the larger arbitrage and auxiliary service profits. However, the larger cycle aging cost caused by greater discharging/charging power could not cover the cycle aging cost of BESS sufficiently. BESS under the proposed model would ensure that the marginal cost of cycle aging does not exceed the marginal market profits from arbitrage and reserve. Accordingly, the annual total profits are more and cycle aging are less as the number of segments increases. The differences between 8-segment and 64-segment could be ignored because the increasing number of segments estimates cycle aging cost accurate enough.

In order to analyze the impact of the proposed method on battery expectancy life, the battery expectancy life can be formulated [26]:

$$L = \frac{Q^{Loss}}{Q^{cal} + Q^{cycle}} \quad (31)$$

where L is the battery expectancy life; Q^{Loss} is the total aging percentage when the battery reaches EOL. Generally, it is set to 80% [12]; Q^{cal} is the annual calendar aging of battery; Q^{cycle} is the annual cycle aging of the battery. For example, the shelf life of BESS is assumed to be 10 years and Q^{Loss} is assumed to be 80%. Therefore, the Q^{cal} is 8% per year. After introducing the Q^{cycle} , the expectancy life would be smaller than the situation when only considering the annual calendar aging of the battery.

Table 4 shows the battery expectancy life under different numbers of segments in the energy and auxiliary service market. The findings observed from Fig. 6 are still held. The proposed model can effectively improve the longevity

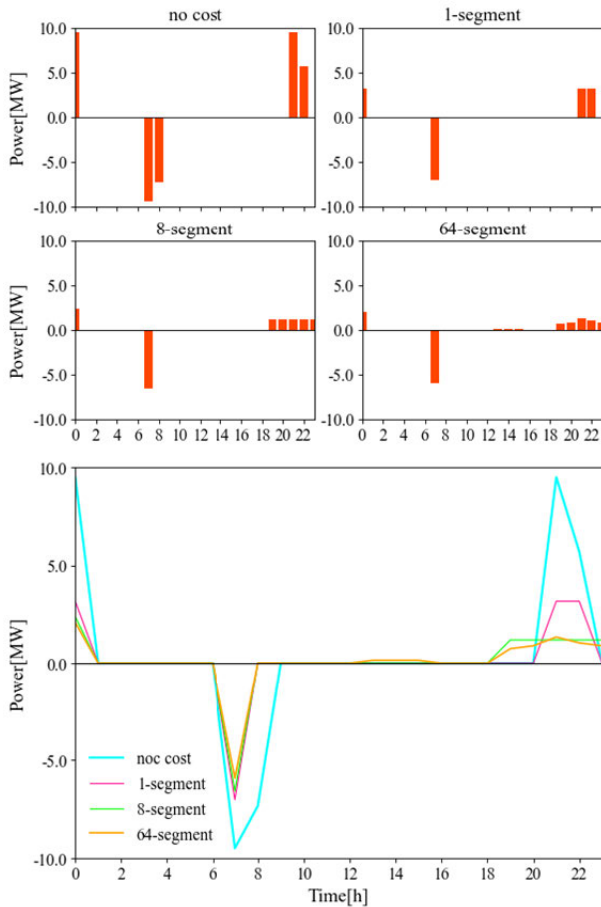


FIGURE 6. (a) The discharging/charging power of BESS in the energy and auxiliary service market. (b) The discharging power in the same axis. The positive and negative value represents discharging and charging power, respectively.

TABLE 4. Battery expectancy life under different numbers of segments in the energy and auxiliary service market.

	No Cost	1-segment	8-segment	16-segment	144-segment
Battery Expectancy Life/year	1.7	8.0	8.6	8.9	8.9

of BESS by approximately 7.5%~11% than the fixed cost model of the battery.

4) SENSITIVITY ANALYSIS
a: THE NUMBER OF SEGMENTS

The increment segments make the estimation of cycle aging cost more accurate. However, the profits and cycle aging cost of BESSs also depend on the initial SOC. While BESS with lower initial SOC has more capacity to arbitrage, the arbitrage profits may increase. The profits from auxiliary service may increase when the initial SOC of BESS is high due to more energies has been stored in the battery. The trend of total profits is uncertain, because the cycle aging cost may increase

with the arbitrage. To test the robustness of the conclusions for some key assumptions. We conduct sensitivity analysis for two critical parameters on the overall profits and cycle aging: a) we vary the initial SOC of BESS from 15% to 95% by an interval of 10%, b) we vary the number of segments from 1 to 144. The comparisons of overall profits and cycle aging are summarized in Fig. 7, Fig. 8, and Table 5.

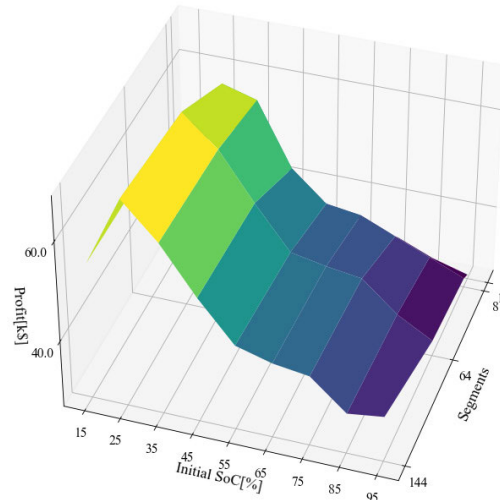


FIGURE 7. The annual profits with different initial SOC of BESS under the proposed model.

As expected, more segments lead to the increase of profits in the same initial in Fig. 7. This is also true for BESSs during the optimization dispatch. Larger energy capacity for BESS to arbitrage with lower SOC, which improves the profits. Oppositely, profits are lower as the decreasing initial SOC of BESS. Moreover, the cycle aging cost of BESS is increasing as the initial SOC decreases in Fig. 8. Additionally, too high initial SOC decreases the ability of BESS to arbitrage despite it can reduce the cycle aging of the battery.

Table 5 shows the annual profits and cycle aging with different initial SOC and numbers of segments compared with 15% SOC under the fixed cost battery model. It is necessary to select proper numbers of segments depending on the actual optimization requirement

b: THE REPLACEMENT COST

The replacement cost determines the aging cost derived from arbitrage and reserve. Higher replacement costs would make BESSs tend to arbitrage more conservative. While BESSs are with lower replacement costs, the aging cost in the same discharging/charging power would also be lower. However, the battery life aging would also be accelerated with lower replacement costs. The results under different replacement costs need to be explored.

To test the influence of replacement costs, we conduct the simulation with different replacement costs under the 64-segment model. The comparisons of profits and expectancy life of the battery are shown in Fig. 9 and Table 6.

TABLE 5. The annual profits and cycle aging with different initial SOC and numbers of segments compared with 15% SOC under fixed cost battery model.

Initial SOC	Annual Profit Improvement (%)			Annual Cycle Aging (%)		
	8-segment	64-segment	144-segment	8-segment	64-segment	144-segment
15%	17	27	27	1.30	0.98	0.97
25%	39	56	60	1.40	1.00	1.00
35%	34	41	43	1.10	0.96	0.96
45%	4.5	19	22	1.10	0.96	0.95
55%	-9.7	0.9	3.1	0.98	0.96	0.95
65%	-19	-4.2	-1.7	0.97	0.95	0.95
75%	-24	-6.6	-4.0	0.96	0.95	0.95
85%	-31	-21	-18	0.96	0.93	0.92

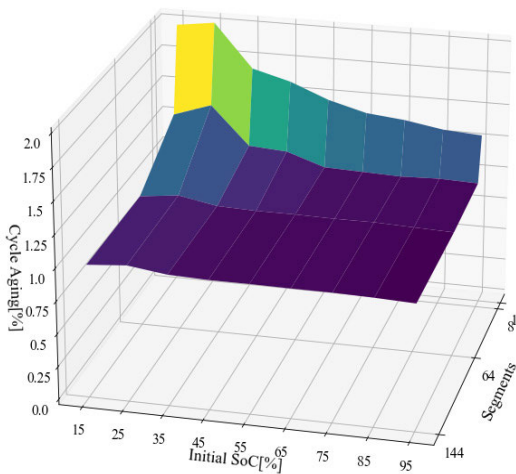


FIGURE 8. The annual cycle aging with different initial SOC of BESS under the proposed model.

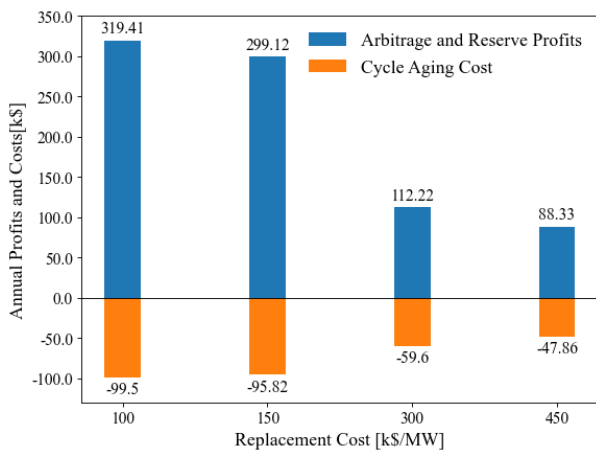


FIGURE 9. The annual cycle aging cost and arbitrage and reserve profits with different replacement costs of BESS under the 64-segment model.

The arbitrage and reserve profits decreased from \$319.41 thousand under \$ 100 thousand/MW to \$88.33 thousand under \$ 450 thousand/MW. The BESS would arbitrage more

TABLE 6. The annual total profits and battery expectancy life with different replacement costs of BESS under the 64-segment model.

Replacement Cost/(k\$/MW)	100	150	300	450
Annual Total Profits/k\$	219.91	203.28	52.62	40.47
Battery Expectancy Life/year	4.4	6.7	8.6	9.1

aggressively because of the lower replacement costs. Further, the total profits are also higher at lower replacement costs.

The total profits increased from 40.47 with \$450 thousand/MW to \$ 219.91 thousand/MW. However, frequently discharging/charging would lead to more aging of battery as expected. The battery expectancy life decreased from 9.1 years to 4.4 as the replacement increased. Consequently, lower replacement costs would have an increment on the annual total profits but would accelerate the degradation of the battery, which may result in more payments in long-time-scale optimization dispatch.

V. CONCLUSION

This study proposed a cycle aging cost model of the ESS considering battery life degradation. First, based on the Arrhenius law, the single-variable battery cycle aging model was proposed by eliminating the cycle number to easily estimate one-cycle battery degradation. Second, the cycle aging of the battery was associated with discharging power, which is derived from the single-variable model. Third, the piecewise linear model was used to linearize the ESS cycle aging cost model. Based on the optimization simulations on the day-ahead energy and auxiliary service market, the various numbers of segments demonstrated the effectiveness and accuracy of the proposed model, the relative error is less than 5% between the estimation and actual cycle aging of BESS under small numbers of segments. Next, the annual profits and SoH revealed that the proposed cycle aging cost model of the battery can considerably improve ESS profitability by 27% and longevity by 11% at least.

The proposed method in this study is easy to implement and suitable for calculating the battery cycle aging cost for various types of batteries. Based on this battery degradation model, further research on multi-scenario real-time ESS dispatch should be performed in the future.

REFERENCES

- [1] M. Arbabzadeh, R. Sioshansi, J. X. Johnson, and G. A. Keoleian, "The role of energy storage in deep decarbonization of electricity production," *Nature Commun.*, vol. 10, no. 1, p. 3413, Dec. 2019, doi: [10.1038/s41467-019-11161-5](https://doi.org/10.1038/s41467-019-11161-5).
- [2] B. Li, Z. Ma, P. Hidalgo-Gonzalez, A. Latham, N. Fedorova, G. He, H. Zhong, M. Chen, and D. M. Kammen, "Modeling the impact of EVs in the Chinese power system: Pathways for implementing emissions reduction commitments in the power and transportation sectors," *Energy Policy*, vol. 149, Feb. 2021, Art. no. 111962, doi: [10.1016/j.enpol.2020.111962](https://doi.org/10.1016/j.enpol.2020.111962).
- [3] M. Cucuzzella, T. Bouman, K. Kosaraju, G. Schuitema, N. H. Lemmen, S. J. Zawadzki, C. Fischione, L. Steg, and J. M. Scherpen, "Distributed control of DC grids: Integrating prosumers' motives," *IEEE Trans. Power Syst.*, early access, Sep. 1, 2021, doi: [10.1109/TPWRS.2021.3109024](https://doi.org/10.1109/TPWRS.2021.3109024).
- [4] L. Zheng, Z. Wang, S. Lv, J. Song, and M. Tian, "Hierarchical operation control of multi-energy storage in DC microgrid based on state of charge," *Power Syst.*, vol. 45, no. 3, pp. 1006–1015, 2021.
- [5] J. Wang, J. Qin, H. Zhong, R. Rajagopal, Q. Xia, and C. Kang, "Reliability value of distributed solar+storage systems amidst rare weather events," *IEEE Trans. Smart Grid*, vol. 10, no. 4, pp. 4476–4486, Jul. 2019, doi: [10.1109/TSG.2018.2861227](https://doi.org/10.1109/TSG.2018.2861227).
- [6] Y. Zhang, Y. Xu, H. Yang, Z. Y. Dong, and R. Zhang, "Optimal whole-life-cycle planning of battery energy storage for multi-functional services in power systems," *IEEE Trans. Sustain. Energy*, vol. 11, no. 4, pp. 2077–2086, Oct. 2020, doi: [10.1109/TSTE.2019.2942066](https://doi.org/10.1109/TSTE.2019.2942066).
- [7] Y. Shi, B. Xu, D. Wang, and B. Zhang, "Using battery storage for peak shaving and frequency regulation: Joint optimization for superlinear gains," *IEEE Trans. Power Syst.*, vol. 33, no. 3, pp. 2882–2894, May 2018, doi: [10.1109/TPWRS.2017.2749512](https://doi.org/10.1109/TPWRS.2017.2749512).
- [8] M. Zheng, C. J. Meinrenken, and K. S. Lackner, "Smart households: Dispatch strategies and economic analysis of distributed energy storage for residential peak shaving," *Appl. Energy*, vol. 147, pp. 246–257, Jun. 2015, doi: [10.1016/j.apenergy.2015.02.039](https://doi.org/10.1016/j.apenergy.2015.02.039).
- [9] H. S. Dhiman, D. Deb, S. M. Muyeen, and A. Abraham, "Machine intelligent forecasting based penalty cost minimization in hybrid wind-battery farms," *Int. Trans. Electr. Energy Syst.*, vol. 31, no. 9, pp. 1–15, Sep. 2021, doi: [10.1002/2050-7038.13010](https://doi.org/10.1002/2050-7038.13010).
- [10] P. Patel and D. Deb, "Battery state of charge based algorithm for optimal wind farm power management," in *Proc. 6th Int. Conf. Comput. Appl. Electr. Eng.-Recent Adv. (CERA)*, Oct. 2017, pp. 42–46, doi: [10.1109/CERA.2017.8343298](https://doi.org/10.1109/CERA.2017.8343298).
- [11] H. Shuai and H. He, "Online scheduling of a residential microgrid via Monte-Carlo tree search and a learned model," *IEEE Trans. Smart Grid*, vol. 12, no. 2, pp. 1073–1087, Mar. 2021, doi: [10.1109/TSG.2020.3035127](https://doi.org/10.1109/TSG.2020.3035127).
- [12] A. E. Mejdoubi, A. Oukaour, and H. Chaoui, "State-of-charge and state-of-health lithium-ion batteries' diagnosis according to surface temperature variation," *IEEE Trans. Ind. Electron.*, vol. 63, no. 4, pp. 2391–2402, Apr. 2016, doi: [10.1109/TIE.2015.2509916](https://doi.org/10.1109/TIE.2015.2509916).
- [13] V. K. Prajapati and V. Mahajan, "Reliability assessment and congestion management of power system with energy storage system and uncertain renewable resources," *Energy*, vol. 215, Jan. 2021, Art. no. 119134, doi: [10.1016/j.energy.2020.119134](https://doi.org/10.1016/j.energy.2020.119134).
- [14] M. Ecker, N. Nieto, S. Käbitz, J. Schmalstieg, H. Blanke, A. Warnecke, and D. U. Sauer, "Calendar and cycle life study of Li(NiMnCo)O₂-based 18650 lithium-ion batteries," *J. Power Sources*, vol. 248, pp. 839–851, Feb. 2014, doi: [10.1016/j.jpowsour.2013.09.143](https://doi.org/10.1016/j.jpowsour.2013.09.143).
- [15] M. Chawla, R. Naik, R. Burra, and H. Wiegman, "Utility energy storage life degradation estimation method," in *Proc. IEEE Conf. Innov. Technol. Efficient Reliable Electr. Supply*, Sep. 2010, pp. 302–308.
- [16] A. Eddahech, O. Briat, E. Woignard, and J. M. Vinassa, "Remaining useful life prediction of lithium batteries in calendar ageing for automotive applications," *Microelectron. Rel.*, vol. 52, no. 9, pp. 2438–2442, Sep. 2012, doi: [10.1016/j.microrel.2012.06.085](https://doi.org/10.1016/j.microrel.2012.06.085).
- [17] Z. Li, L. Lu, M. Ouyang, and Y. Xiao, "Modeling the capacity degradation of LiFePO₄/graphite batteries based on stress coupling analysis," *J. Power Sources*, vol. 196, no. 22, pp. 9757–9766, Nov. 2011, doi: [10.1016/j.jpowsour.2011.07.080](https://doi.org/10.1016/j.jpowsour.2011.07.080).
- [18] S. Grolleau, A. Delaille, H. Gualous, P. Gyan, R. Revel, J. Bernard, E. Redondo-Iglesias, and J. Peter, "Calendar aging of commercial graphite/LiFePO₄ cell—Predicting capacity fade under time dependent storage conditions," *J. Power Sources*, vol. 255, pp. 450–458, Jun. 2014, doi: [10.1016/j.jpowsour.2013.11.098](https://doi.org/10.1016/j.jpowsour.2013.11.098).
- [19] J. Wang, P. Liu, J. Hicks-Garner, E. Sherman, S. Soukiazian, M. Verbrugge, H. Tataria, J. Musser, and P. Finamore, "Cycle-life model for graphite-LiFePO₄ cells," *J. Power Sources*, vol. 196, no. 8, pp. 3942–3948, 2011, doi: [10.1016/j.jpowsour.2010.11.134](https://doi.org/10.1016/j.jpowsour.2010.11.134).
- [20] I. Laresgoiti, S. Käbitz, M. Ecker, and D. U. Sauer, "Modeling mechanical degradation in lithium ion batteries during cycling: Solid electrolyte interphase fracture," *J. Power Sources*, vol. 300, pp. 112–122, Dec. 2015, doi: [10.1016/j.jpowsour.2015.09.033](https://doi.org/10.1016/j.jpowsour.2015.09.033).
- [21] T. Xu, W. Wang, M. L. Gordin, D. Wang, and D. Choi, "Lithium-ion batteries for stationary energy storage," *JOM*, vol. 62, no. 9, pp. 24–30, Sep. 2010, doi: [10.1007/s11837-010-0131-6](https://doi.org/10.1007/s11837-010-0131-6).
- [22] M. Safari, M. Morcrette, A. Teyssoit, and C. Delacourt, "Multimodal physics-based aging model for life prediction of li-ion batteries," *J. Electrochem. Soc.*, vol. 156, no. 3, p. A145, 2009, doi: [10.1149/1.3043429](https://doi.org/10.1149/1.3043429).
- [23] Z. Song, X.-G. Yang, N. Yang, F. P. Delgado, H. Hofmann, and J. Sun, "A study of cell-to-cell variation of capacity in parallel-connected lithium-ion battery cells," *eTransportation*, vol. 7, Feb. 2021, Art. no. 100091, doi: [10.1016/j.etrans.2020.100091](https://doi.org/10.1016/j.etrans.2020.100091).
- [24] J. Wang, S. Soukiazian, M. Verbrugge, H. Tataria, D. Coates, D. Hall, and P. Liu, "Active lithium replenishment to extend the life of a cell employing carbon and iron phosphate electrodes," *J. Power Sources*, vol. 196, no. 14, pp. 5966–5969, Jul. 2011, doi: [10.1016/j.jpowsour.2011.02.087](https://doi.org/10.1016/j.jpowsour.2011.02.087).
- [25] J. Schmalstieg, S. Käbitz, M. Ecker, and D. U. Sauer, "A holistic aging model for Li(NiMnCo)O₂ based 18650 lithium-ion batteries," *J. Power Sources*, vol. 257, pp. 325–334, Jul. 2014, doi: [10.1016/j.jpowsour.2014.02.012](https://doi.org/10.1016/j.jpowsour.2014.02.012).
- [26] B. Xu, J. Zhao, T. Zheng, E. Litvinov, and D. S. Kirschen, "Factoring the cycle aging cost of batteries participating in electricity markets," *IEEE Trans. Power Syst.*, vol. 33, no. 2, pp. 2248–2259, Mar. 2018, doi: [10.1109/TPWRS.2017.2733339](https://doi.org/10.1109/TPWRS.2017.2733339).
- [27] I. Bloom, B. W. Cole, J. J. Sohn, S. A. Jones, E. G. Polzin, V. S. Battaglia, G. L. Henriksen, C. Motloch, R. Richardson, T. Unkelhaeuser, and D. Ingersoll, "An accelerated calendar and cycle life study of Li-ion cells," *J. Power Sources*, vol. 101, no. 2, pp. 238–247, Oct. 2001, doi: [10.1016/S0378-7753\(01\)00783-2](https://doi.org/10.1016/S0378-7753(01)00783-2).
- [28] H. S. Dhiman and D. Deb, "Wake management based life enhancement of battery energy storage system for hybrid wind farms," *Renew. Sustain. Energy Rev.*, vol. 130, Sep. 2020, Art. no. 109912, doi: [10.1016/j.rser.2020.109912](https://doi.org/10.1016/j.rser.2020.109912).
- [29] B. Xu, A. Oudalov, A. Ulbig, G. Andersson, and D. S. Kirschen, "Modeling of lithium-ion battery degradation for cell life assessment," *IEEE Trans. Smart Grid*, vol. 9, no. 2, pp. 1131–1140, Mar. 2018, doi: [10.1109/TSG.2016.2578950](https://doi.org/10.1109/TSG.2016.2578950).
- [30] G. He, Q. Chen, P. Moutis, S. Kar, and J. F. Whitacre, "An intertemporal decision framework for electrochemical energy storage management," *Nature Energy*, vol. 3, no. 5, pp. 404–412, May 2018, doi: [10.1038/s41560-018-0129-9](https://doi.org/10.1038/s41560-018-0129-9).
- [31] H. S. Dhiman and D. Deb, "Fuzzy TOPSIS and fuzzy COPRAS based multi-criteria decision making for hybrid wind farms," *Energy*, vol. 202, Jul. 2020, Art. no. 117755, doi: [10.1016/j.energy.2020.117755](https://doi.org/10.1016/j.energy.2020.117755).
- [32] B. S. Malepati, D. Vijay, D. Deb, and K. Manjunath, "Parameter validation to ascertain voltage of Li-ion battery through adaptive control," *Innov. Infrastruct.*, pp. 21–31, 2019.
- [33] P. Patel, A. Shandilya, and D. Deb, "Optimized hybrid wind power generation with forecasting algorithms and battery life considerations," in *Proc. IEEE Power Energy Conf. Illinois (PECI)*, Feb. 2017, pp. 1–6, doi: [10.1109/PECI.2017.7935735](https://doi.org/10.1109/PECI.2017.7935735).
- [34] Q. Li, S. S. Choi, Y. Yuan, and D. L. Yao, "On the determination of battery energy storage capacity and short-term power dispatch of a wind farm," *IEEE Trans. Sustain. Energy*, vol. 2, no. 2, pp. 148–158, Apr. 2011, doi: [10.1109/TSTE.2010.2095434](https://doi.org/10.1109/TSTE.2010.2095434).
- [35] D. L. Yao, S. S. Choi, K. J. Tseng, and T. T. Lie, "Determination of short-term power dispatch schedule for a wind farm incorporated with dual-battery energy storage scheme," *IEEE Trans. Sustain. Energy*, vol. 3, no. 1, pp. 74–84, Jan. 2012, doi: [10.1109/TSTE.2011.2163092](https://doi.org/10.1109/TSTE.2011.2163092).

[36] G. Hug, S. Kar, and C. Wu, "Consensus + innovations approach for distributed multiagent coordination in a microgrid," *IEEE Trans. Smart Grid*, vol. 6, no. 4, pp. 1893–1903, Jul. 2015, doi: [10.1109/TSG.2015.2409053](https://doi.org/10.1109/TSG.2015.2409053).

[37] A. Khatamianfar, M. Khalid, A. V. Savkin, and V. G. Agelidis, "Improving wind farm dispatch in the Australian electricity market with battery energy storage using model predictive control," *IEEE Trans. Sustain. Energy*, vol. 4, no. 3, pp. 745–755, Jul. 2013, doi: [10.1109/TSTE.2013.2245427](https://doi.org/10.1109/TSTE.2013.2245427).

[38] J. Qin, Y. Wan, X. Yu, F. Li, and C. Li, "Consensus-based distributed coordination between economic dispatch and demand response," *IEEE Trans. Smart Grid*, vol. 10, no. 4, pp. 3709–3719, Jul. 2019, doi: [10.1109/TSG.2018.2834368](https://doi.org/10.1109/TSG.2018.2834368).

[39] G. He, S. Kar, J. Mohammadi, P. Moutis, and J. F. Whitacre, "Power system dispatch with marginal degradation cost of battery storage," *IEEE Trans. Power Syst.*, vol. 36, no. 4, pp. 3552–3562, Jul. 2021, doi: [10.1109/TPWRS.2020.3048401](https://doi.org/10.1109/TPWRS.2020.3048401).

[40] M. Ross, C. Abbey, F. Bouffard, and G. Joos, "Microgrid economic dispatch with energy storage systems," *IEEE Trans. Smart Grid*, vol. 9, no. 4, pp. 3039–3047, Jul. 2018, doi: [10.1109/TSG.2016.2624756](https://doi.org/10.1109/TSG.2016.2624756).

[41] A. Cherukuri and J. Cortes, "Distributed coordination of DERs with storage for dynamic economic dispatch," *IEEE Trans. Autom. Control*, vol. 63, no. 3, pp. 835–842, Mar. 2018, doi: [10.1109/TAC.2017.2731809](https://doi.org/10.1109/TAC.2017.2731809).

[42] J. Tant, F. Geth, D. Six, P. Tant, and J. Driesen, "Multiobjective battery storage to improve PV integration in residential distribution grids," *IEEE Trans. Sustain. Energy*, vol. 4, no. 1, pp. 182–191, Jan. 2013, doi: [10.1109/TSTE.2012.2211387](https://doi.org/10.1109/TSTE.2012.2211387).

[43] G. He, Q. Chen, C. Kang, P. Pinson, and Q. Xia, "Optimal bidding strategy of battery storage in power markets considering performance-based regulation and battery cycle life," *IEEE Trans. Smart Grid*, vol. 7, no. 5, pp. 2359–2367, Sep. 2016, doi: [10.1109/TSG.2015.2424314](https://doi.org/10.1109/TSG.2015.2424314).

[44] Y. Wang, *Research on Modeling, State Estimation and Management Strategy of Power Lithium-Ion Batteries*. Hefei, China: Univ. Science and Technology of China, 2017.

[45] R. Spotnitz, "Simulation of capacity fade in lithium-ion batteries," *J. Power Sources*, vol. 113, pp. 72–80, Jan. 2003, doi: [10.1016/S0378-7753\(02\)00490-1](https://doi.org/10.1016/S0378-7753(02)00490-1).

[46] Y. J. A. Zhang, C. Zhao, W. Tang, and S. H. Low, "Profit-maximizing planning and control of battery energy storage systems for primary frequency control," *IEEE Trans. Smart Grid*, vol. 9, no. 2, pp. 712–723, Mar. 2018, doi: [10.1109/TSG.2016.2562672](https://doi.org/10.1109/TSG.2016.2562672).

[47] Q. Liu, M. Liu, and W. Lu, "Control method for battery energy storage participating in frequency regulation market considering degradation cost," *Power Syst.*, vol. 45, no. 8, pp. 3043–3051, 2021.



BO LI (Student Member, IEEE) received the B.S. degree in electrical engineering from Guangxi University, Nanning, China, in 2016. He is currently pursuing the Ph.D. degree with Chongqing University, Chongqing, China.

His research interests include power system optimization and planning, energy policy, and renewable energy integration.



XIAO QIAN is currently a Senior Engineer with State Grid Zhejiang Electric Power Company, China.

His research interests include energy storage systems and power systems planning.



SHUJUN ZHANG received the B.S. and M.S. degrees from Shanghai Jiao Tong University, Shanghai, China.

She is currently a Senior Engineer with State Grid Zhejiang Electric Power Company, China. Her research interests include power system optimization and planning, power production planning, and electric power technology management.



XIANGJIN WANG received the B.S. and M.S. degrees in electrical engineering from the Hefei University of Technology, Hefei, Anhui, China, in 2014 and 2017, respectively. He is currently an Engineer with the State Grid Zhejiang Electric Power Research Institute, Hangzhou, Zhejiang, China. His research interests include energy management and optimization sizing of battery energy.



LEIQI ZHANG received the B.Eng. and Ph.D. degrees from the College of Electrical Engineering, Zhejiang University, Hangzhou, China, in July 2012 and July 2017, respectively.

He is currently an Engineer with the State Grid Zhejiang Electric Power Research Institute, China. His research interests include distributed generation and control.



XUESONG ZHANG received the Ph.D. degree from the Department of Electrical Engineering, Zhejiang University, Hangzhou, China, in July 2006. He is currently a Senior Engineer with the State Grid Zhejiang Electric Power Research Institute, China. His research interests include energy storage systems and microgrids.



YANJIE YU received the B.S. degree in electrical engineering from the Harbin University of Science and Technology, Harbin, China, in 2020. He is currently pursuing the master's degree with Chongqing University, Chongqing, China.

His research interests include microgrid dispatch and distributed optimization.



MINYOU CHEN (Senior Member, IEEE) received the M.Sc. degree from Chongqing University, Chongqing, China, in 1987, and the Ph.D. degree in automatic control and systems engineering from The University of Sheffield, Sheffield, U.K., in 1998.

He is currently a Professor of electrical engineering with the School of Electrical Engineering, Chongqing University. His main research interests include intelligent modeling and control, multi-smart grid, and reliability of power electronic equipment.